DALTON

The reaction of HCl with $[MoH_3(CCBu^t)(Ph_2PCH_2CH_2PPh_2)_2]$: enforced protonation at the metal gives an alkyne †

Richard A. Henderson* and Kay E. Oglieve

John Innes Centre, Nitrogen Fixation Laboratory, Norwich Research Park, Colney, Norwich NR4 7UH, UK

The reaction of anhydrous HCl with $[MoH_3(CCBu^t)(dppe)_2]$ in tetrahydrofuran produced $[MoH_2Cl_2(dppe)_2]$ together with dihydrogen and Bu^tCCH. Initial protonation of $[MoH_3(CCBu^t)(dppe)_2]$ generates an equilibrium mixture of $[MoH_3(CCHBu^t)(dppe)_2]^+$ and $[MoH_4(CCBu^t)(dppe)_2]^+$, in which the predominant species is the vinylidene complex. However, it is $[MoH_4(CCBu^t)(dppe)_2]^+$ which is the more reactive of the two protonated species, since intramolecular reductive coupling of a hydride and alkynyl ligand in this complex is more rapid than the analogous coupling of two hydride ligands in $[MoH_3(CCHBu^t)(dppe)_2]^+$, and thus the reaction proceeds along the pathway involving $[MoH_3(\eta^2\text{-}CHCBu^t)(dppe)_2]^+$. Further protonation of the metal in $[MoH_3(\eta^2\text{-}CHCBu^t)(dppe)_2]^+$ labilises the site to dissociation of first dihydrogen, then Bu^tCCH, and subsequent binding of chloride produces $[MoH_2Cl_2(dppe)_2]$. The general factors associated with the protonation of alkynyl complexes at either (*i*) the metal to give an alkyne or (*ii*) the alkynyl ligand to give an alkylidyne complex are discussed.

Studies on the protonation mechanisms of hydrocarbon residues bound to electron-rich metal sites such as $\{M(dppe)_2\}$ (M = Mo or W, dppe = $Ph_2PCH_2CH_2PPh_2$)[1] have led to an understanding of the factors which define whether it is a carbon site or the metal which is protonated preferentially and the way in which this controls the products of the reactions. Recently we have extended this work to alkynyl complexes. We have reported studies on the reaction between anhydrous HCl and $[MoH_2(CCBu^t)_2(depe)_2]$ (depe = $Et_2PCH_2CH_2PEt_2$)[2] in tetrahydrofuran (thf) to form the alkylidyne complex, $[MoH(Cl)(CCH_2Bu^t)(depe)_2]^+$, and demonstrated three important mechanistic features associated with this reaction: (*i*) the unsaturated carbon atom remote from the metal (hereafter referred to as C_β) on the alkynyl residue is the most rapidly protonated site, with protonation of the metal being at least 500 times slower; (*ii*) two protons must be added to labilise the site towards dissociation and (*iii*) an intramolecular reductive-coupling step is required after the addition of the first proton, to facilitate the second protonation step. In this paper we report that the reaction of anhydrous HCl with $[MoH_3(CCBu^t)(dppe)_2]$ forms no alkylidyne complex, but rather an alkyne is produced. Mechanistic studies show this is because rapid protonation at the C_β site of the alkynyl ligand gives a species which can only slowly react further with acid (to give an alkylidyne), whilst the kinetically and thermodynamically less-favourable protonation of the metal results in a more labile species capable of producing alkyne. Herein we discuss the general factors which discriminate between these two protonation pathways, as summarised in Scheme 1.

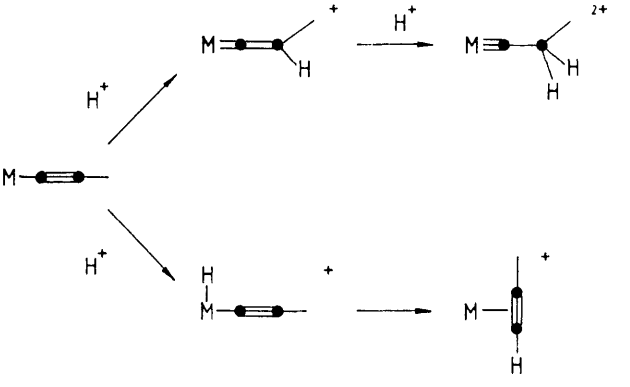

Scheme 1 Products formed by protonation of alkynyl complexes: alkylidyne complex formed by protonation at C_β of the alkynyl ligand (top) and alkyne species formed by protonation at the metal (bottom)

Experimental

All manipulations in this work were routinely performed under an atmosphere of argon or dinitrogen using standard vacuum-line or syringe techniques as appropriate. Solvents were distilled under an atmosphere of dry dinitrogen, from the necessary drying agents, immediately prior to use: tetrahydrofuran (sodium–benzophenone); methanol (magnesium methoxide) and diethyl ether (sodium).

Typical dihydrogen analysis

In a typical experiment the amount of dihydrogen evolved in the reaction of $[MoH_3(CCBu^t)(dppe)_2]$ with anhydrous HCl was determined in the following manner. The complex $[MoH_3(CCBu^t)(dppe)_2]$ (0.0488 g, 10 mmol) was weighed into a flask (25 cm^3) which was then sealed with a rubber septum. The flask was evacuated through a needle connection and filled with an atmosphere of argon. In a separate Schlenk flask, freshly distilled thf was degassed and stirred for 30 min under argon. Tetrahydrofuran (5 cm^3) was transferred on top of the complex using a syringe and needle. After the complex had dissolved a known concentration of HCl (20–100 mmol dm^{-3}, prepared by mixing equimolar amounts of MeOH and $SiMe_3Cl$) was introduced through the septum using a syringe and needle.

A control solution of $[MoH_3(CCBu^t)(dppe)_2]$ (0.0488 g, 10 mmol dm^{-3}) in thf (5 cm^3) was also prepared. The liberated gas was analysed by GLC after 2 h. No dihydrogen was detected.

The dihydrogen gas was analysed quantitatively by GLC (molecular sieve 80–100 mesh column operating at 60 °C), using

† *Supplementary data available* (No. SUP 57157, 3 pp.): k_{obs} values. See Instructions for Authors, *J. Chem. Soc., Dalton Trans.*, 1996, Issue 1.

Table 1 Elemental analyses and spectroscopic characterisation of complexes, including products of reactions

Complex	Analysis[a] (%) C	H	IR[b]/cm^{-1}	NMR[c] ^{1}H	^{31}P	^{13}C
$[MoH_3(CCBu^t)(dppe)_2]$[d]	71.5 (71.3)	5.9 (6.1)	1960 ν(CC) 1810 ν(MoH)	−4.1 (qnt, MoH, J_{HP} = 29.5) 1.3 (s, CMe_3)	−57 (s)	15.1 (CMe_3) 22.8 (PCH_2) 32.0 (CMe_3) 116.2 ($CCCMe_3$) 123–130 (m, Ph) 146.3 ($CCCMe_3$)
$[MoH_2Cl_2(dppe)_2]$[d]	53.9 (53.9)	5.0 (5.2)	1880 ν(MoH)	−4.5 (qnt, MoH, J_{HP} = 45)	−70.4 (t) −97.2 (t) J_{PP} = 10	
$[MoF(CCH_2Bu^t)(dppe)_2]BF_4$[e]	53.3 (53.7)	5.4 (5.5)	1080 ν(BF)			

[a] Calculated values shown in parentheses. [b] Recorded as Nujol mulls, all bands strong. [c] Proton and ^{13}C peaks relative to $SiMe_4$, ^{31}P relative to $P(OMe)_3$; s = singlet, t = triplet, qnt = quintet, m = multiplet; *J* in Hz. [d] Proton NMR spectrum also shows peaks associated with dppe ligands at δ *ca.* 6.9–7.6 (m, Ph) and *ca.* 2.5 (m, PCH_2). [e] Complex is paramagnetic; ^{19}F NMR spectrum shows only δ −153 (s, BF_4), relative to $CFCl_3$.

argon as the carrier gas, with a thermal conductivity detector in a Philips PU 4400 gas chromatograph connected to a PU 4815 computing integrator. Injector and detector temperatures were set to 100 °C. In all GLC experiments the samples were taken into plastic, disposable, syringes. The sample size injected onto the column was 0.1 cm^3. The retention time for dihydrogen was 2.36–2.39 min. It was also analysed using a MassTorr DX mass spectrometer. In the studies with DCl the isotopic composition of the dihydrogen gas was determined by this technique.

Kinetic studies

All the kinetic studies were performed on a Hi-Tech SF-51 spectrophotometer, modified to handle air-sensitive materials.[3] The temperature was maintained at 25.0 °C using a Grant LE8 thermostat tank. The spectrophotometer was interfaced to a Viglen 486 computer *via* an A/D converter. Under all conditions the traces could be fitted satisfactorily by exponentials for at least three half-lives, using a standard curve-fitting program. All rate constants reported are the averages from three duplicate runs the rate and absorbance changes of which differ by less than 5%. A typical trace observed in this study is shown in Fig. 1.

All kinetics were studied under pseudo-first-order conditions with [HCl]/[Mo] > 10:1 in tetrahydrofuran as solvent and using $[NBu^n_4]BF_4$ to maintain a constant ionic strength of 0.1 mol dm^{-3}.

Solutions of anhydrous HCl in thf were prepared by mixing an equimolar amount of $SiMe_3Cl$ and MeOH in the required volume of thf. Typically a stock solution of 0.2 mol dm^{-3} was prepared and more dilute solutions were prepared from this. All solutions were used within 1 h in order to minimise any decomposition of the thf by acid attack. Solutions of DCl were prepared in an analogous fashion, except MeOD was used rather than MeOH.

The dependence of the reaction rate on the concentration of acid was determined by the normal graphical procedures,[4] see Fig. 1.

Preparation of complexes

The complex $[MoH_3(CCBu^t)(dppe)_2]$[5] was prepared by the literature method. Its analytical and spectroscopic characterisation, together with the identification of the product of the reaction with HCl as $[MoH_2Cl_2(dppe)_2]$, and the product of the reaction with $HBF_4{\cdot}OEt_2$ as $[MoF(CCH_2Bu^t)(dppe)_2]BF_4$,[6] are shown in Table 1.

Infrared spectra were recorded on a Perkin-Elmer 883 or a Shimadzu FTIR 8101M spectrophotometer, NMR spectra on a JEOL GX270 spectrometer and UV/VIS absorption spectra on a Shimadzu UV 2101PC spectrophotometer.

Detection of intermediates using low-temperature NMR spectroscopy

The experimental procedure employed to detect intermediates in the reaction between $[MoH_3(CCBu^t)(dppe)_2]$ and HCl in thf using NMR spectroscopy was analogous to that described earlier.[7]

Results and Discussion

Protonation of alkynyl complex gives alkyne

The addition of an excess of anhydrous HCl to a solution of $[MoH_3(CCBu^t)(dppe)_2]$ in thf gives Bu^tCCH, H_2 and $[MoH_2Cl_2(dppe)_2]$, according to the stoichiometry (1). All the

$$[MoH_3(CCBu^t)(dppe)_2] + 2HCl \longrightarrow [MoH_2Cl_2(dppe)_2] + H_2 + Bu^tCCH \quad (1)$$

products shown have been identified. The complex $[MoH_2Cl_2(dppe)_2]$ has been isolated from the reaction mixture and characterised by elemental analysis, IR [ν(MoH) 1880 cm^{-1}], ^{1}H NMR [δ −4.5 (qnt), J_{HP} = 45 Hz, MoH] and ^{31}P-{^{1}H} NMR spectroscopy [δ −70.4 (t), −97.2 (t), J_{PP} = 10 Hz],[8] see Table 1. In addition we have been able to use the diagnostic high-field quintet signal associated with the hydrides in the ^{1}H NMR spectrum, and the pair of triplets observed in the ^{31}P-{^{1}H} NMR spectrum to establish that the same product is formed in solution at all concentrations of HCl.

The amount of dihydrogen released was determined using GLC. The yield of dihydrogen, as defined by equation (1), is essentially quantitative at all concentrations of HCl, $[H_2]/[MoH_3(CCBu^t)(dppe)_2] \geqslant 0.87:1$ {$[MoH_3(CCBu^t)(dppe)_2]$ = 10 mmol dm^{-3}, [HCl] = 20–100 mmol dm^{-3}}.

Finally, Bu^tCCH was identified as a product of the reaction using ^{1}H NMR spectroscopy. After HCl had been bubbled through a thf solution of $[MoH_3(CCBu^t)(dppe)_2]$, peaks identical to those of an authentic sample of the alkyne were observed [δ 1.3(9), s, Me_3CCCH; 2.1(1), s, Me_3CCCH].

When studied on a stopped-flow spectrophotometer (λ = 350–470 nm) reaction (1) clearly occurs in two stages as illustrated by the biphasic absorbance *vs.* time trace shown in Fig. 1. At all acid concentrations the curves can be excellently fitted by two exponentials. This indicates that both stages exhibit a first-order dependence on the complex concentration. This dependence is confirmed by studies at

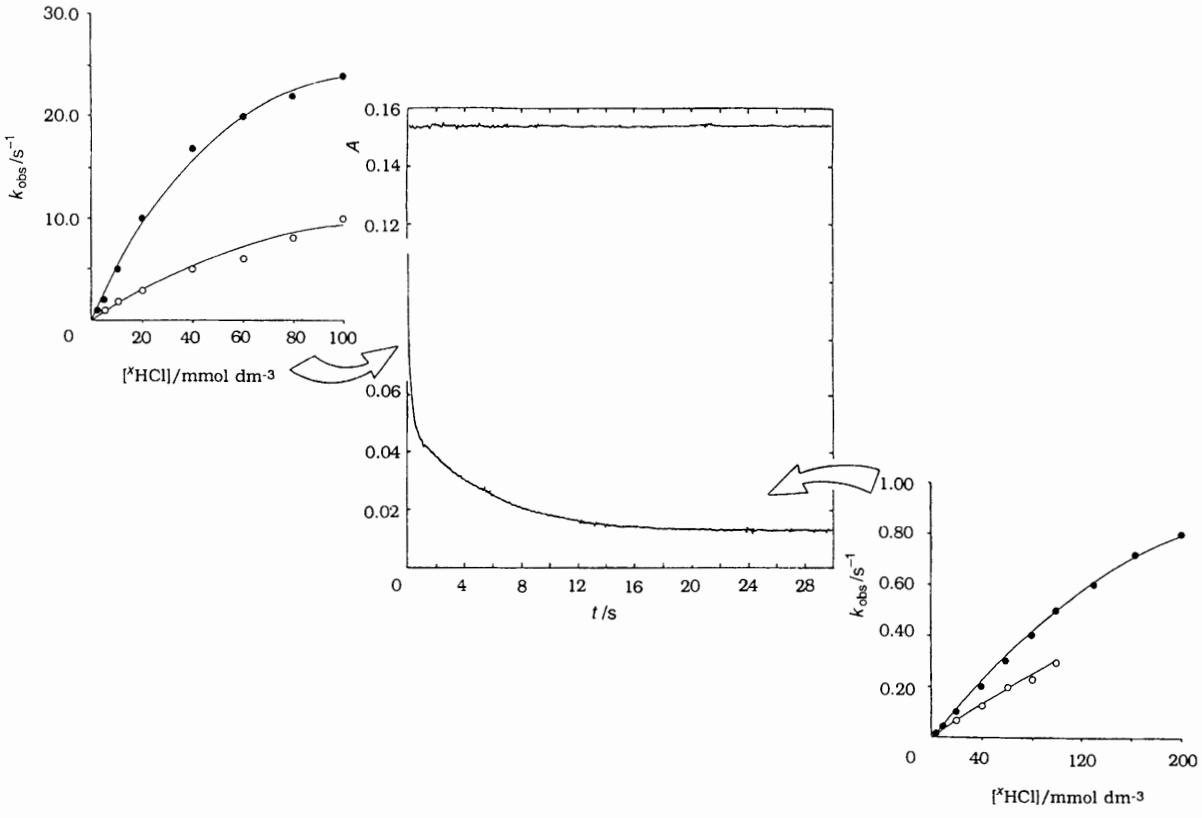

Fig. 1 Stopped-flow absorbance *vs.* time curve for the reaction of $[MoH_3(CCBu^t)(dppe)_2]$ with anhydrous HCl in thf at 25.0 °C, ionic strength = 0.1 mol dm^{-3} ($[NBu^n_4]BF_4$), measured at λ = 450 nm, $[MoH_3(CCBu^t)(dppe)_2]$ = 0.1 mmol dm^{-3} and [HCl] = 40 mmol dm^{-3}. The biphasic curve is excellently fitted by two exponentials using the parameters k_1 = 17 s^{-1}, ΔA_1 = 0.07, k_2 = 0.18 s^{-1}, ΔA_2 = 0.038 and A_∞ = 0.012. The absorbance of $[MoH_3(CCBu^t)(dppe)_2]$ under these conditions is 0.154. The inserts show the dependence of the rate of the reaction for the first stage (left) and the second stage (right) on the concentration of HCl (●) or DCl (○). The curves drawn through the data are those defined by equation (2) using the values defined in the text

[HCl] = 20.0 mmol dm^{-3} over the range of complex concentration, 0.025–0.2 mmol dm^{-3}, where the corresponding observed pseudo-first-order rate constants, $k_{obs}(1)$ = 10.5 ± 0.5 and $k_{obs}(2)$ = 0.11 ± 0.02 s^{-1}, remain constant.

The dependence on the concentration of HCl for both stages is complicated as shown in Fig. 1. In both cases the reaction exhibits a first-order dependence at low concentrations of HCl, whereas at high concentrations the reaction rate becomes independent of the concentration of HCl. Analysis of these data by the usual double-reciprocal graph[9] gives the dependence of the observed pseudo-first-order rate constant on the concentration of HCl shown in equation (2). For the first stage,

$$k_{obs} = \frac{a[HCl]}{1 + b[HCl]} \quad (2)$$

a = (6.0 ± 0.3) × 10^2 dm^3 mol^{-1} s^{-1} and b = 18.0 ± 3.0 dm^3 mol^{-1}, and for the second stage a = 4.93 ± 0.3 dm^3 mol^{-1} s^{-1} and b = 2.46 ± 0.3 dm^3 mol^{-1}.

This kinetic behaviour is consistent with the mechanism shown in Scheme 2. However, before we discuss the details it is important to stress that the configurations and geometries of the intermediates in these reactions are unknown. Only for $[MoH_3(CCBu^t)(dppe)_2]$, the *trans* configuration has been established by X-ray crystallography[5] and the *cis* geometry of $[MoH_2Cl_2(dppe)_2]$ has been defined from ^{31}P-$\{^1H\}$ NMR spectroscopy.[8] A low-temperature ^{31}P-$\{^1H\}$ NMR spectroscopic study on reaction (1) has detected an intermediate (see below), and in this case a *trans* geometry is indicated. For this reason, and for simplicity, the geometries of all intermediates have been represented as *trans* in Scheme 2.

First stage: initial sites of protonation and formation of $[MoH_3(\eta^2\text{-}CHCBu^t)(dppe)_2]^+$. In a previous mechanistic study[2] on the protonation reactions of $[MoH_2(CCBu^t)_2(depe)_2]$ (depe = $Et_2PCH_2CH_2PEt_2$) deuterium-labelling experiments have established that the most rapidly protonated site is C_β of the alkynyl ligand. It seems likely that this is also true for the protonation of $[MoH_3(CCBu^t)(dppe)_2]$ with HCl, as shown in the top line of Scheme 2. Protonation at the alkynyl ligand generates $[MoH_3(CCHBu^t)(dppe)_2]^+$, formally a molybdenum(VI) complex which is consequently unable to be protonated further at either the metal or C_β sites.

The earlier studies[2] on $[MoH_2(CCBu^t)_2(depe)_2]$ showed that, after the initial protonation, addition of a second proton to $[MoH_2(CCHBu^t)(CCBu^t)(depe)_2]^+$ cannot occur until after an intramolecular reductive-coupling step involving a hydrogen atom and the alkynyl residue occurs, to give the formally molybdenum(IV) species $[MoH(CCHBu^t)(\eta^2\text{-}CHCBu^t)(depe)_2]^+$. For the present system it is to be anticipated that the addition of a proton to $[MoH_3(CCHBu^t)(dppe)]^+$ must be preceded by the coupling of two hydride ligands. Consequently, if the coupling step is slow $[MoH_3(CCHBu^t)(dppe)_2]^+$ cannot react further with acid. Under these conditions, competitive protonation of $[MoH_3(CCBu^t)(dppe)]$ to form $[MoH_4(CCBu^t)(dppe)_2]^+$ can occur as shown in the lower portion of Scheme 2. Of course, $[MoH_4(CCBu^t)(dppe)_2]^+$ is another formally molybdenum(VI) species, but the important distinction between the two monoprotonated species $[MoH_3(CCHBu^t)(dppe)_2]^+$ and $[MoH_4(CCBu^t)(dppe)_2]^+$ is that in the latter complex an alkynyl residue is present to which facile intramolecular hydride transfer can occur and generate $[MoH_3(\eta^2\text{-}CHCBu^t)(dppe)_2]^+$, a molybdenum(IV) species now

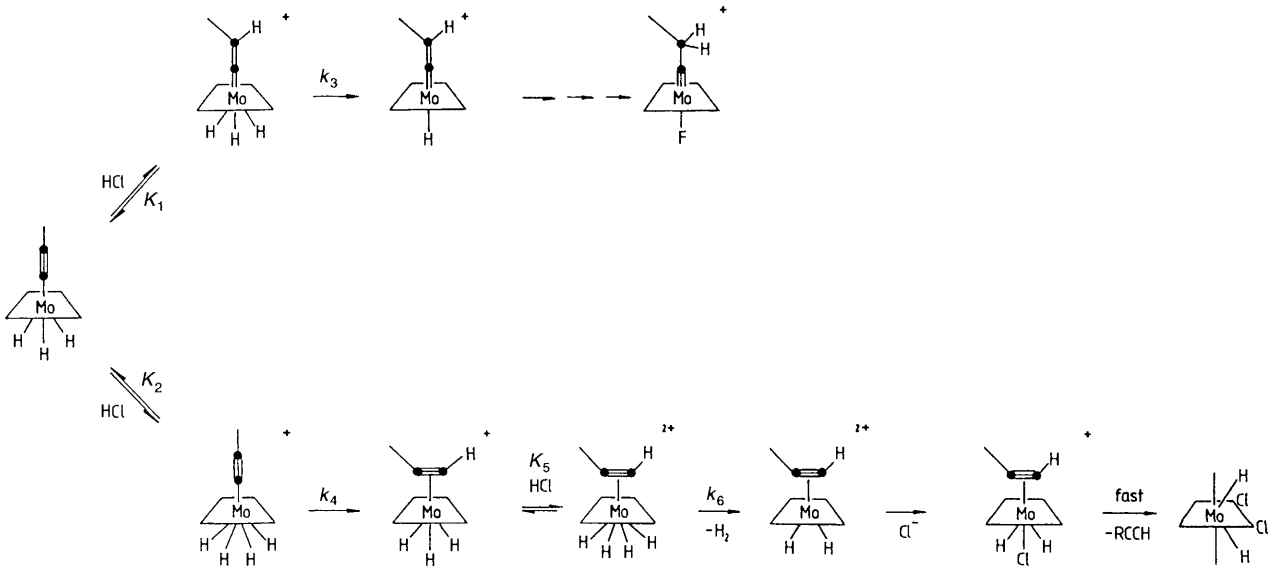

Scheme 2 Mechanism of the reaction of $[MoH_3(CCBu^t)(dppe)_2]$ with anhydrous HCl in thf to form $[MoH_2Cl_2(dppe)_2]$ together with Bu^tCCH and dihydrogen. Phosphine ligands omitted for clarity

capable of further protonation. It is the formation of this alkyne complex which comprises the first stage of the absorbance *vs.* time trace.

Consideration of the mechanism of formation of $[MoH_3(\eta^2\text{-}CHCBu^t)(dppe)_2]^+$ shown in Scheme 2 gives the rate law (3),

$$\frac{d\{[MoH_3(\eta^2\text{-}CHCBu^t)(dppe)_2{}^+] + [MoH_3(CCHBu^t)(dppe)_2{}^+]\}/dt = (k_4K_2 + k_3K_1)[HCl][MoH_3(CCBu^t)(dppe)_2]}{1 + (K_1 + K_2)[HCl]} \quad (3)$$

assuming that: (*i*) both protonation of the C_β site on the alkynyl ligand (K_1) and metal (K_2) are rapidly established equilibria; (*ii*) coupling of hydride and alkynyl in $[MoH_4(CCBu^t)(dppe)_2]^+$ (k_4) is the rate-limiting step in the formation of $[MoH_3(\eta^2\text{-}CHCBu^t)(dppe)_2]^+$ and (*iii*) k_3 is the rate-limiting step associated with the coupling of two hydride ligands in $[MoH_3(CCHBu^t)(dppe)_2]^+$. Equation (3) is identical in form to that observed experimentally [equation (2)] but further simplification is possible. Equation (3) describes the formation of both $[MoH_3(CCHBu^t)(dppe)_2]^+$ (k_3K_1 pathway) and $[MoH_3(\eta^2\text{-}CHCBu^t)(dppe)_2]^+$ (k_4K_2 pathway). However, at all concentrations of HCl stoichiometric amounts of Bu^tCCH and dihydrogen are produced and thus the k_3K_1 term in the numerator can be neglected to give equation (4). Comparison of

$$\frac{d[MoH_3(\eta^2\text{-}CHCBu^t)(dppe)_2{}^+]}{dt} = \frac{k_4K_2[HCl][MoH_3(CCBu^t)(dppe)_2]}{1 + (K_1 + K_2)[HCl]} \quad (4)$$

equations (2) and (4), using the calculated values of a and b for the fast stage gives $k_4K_2 = (6.0 \pm 0.3) \times 10^2$ dm^3 mol^{-1} s^{-1} and $(K_1 + K_2) = 18.0 \pm 3.0$ dm^3 mol^{-1}.

This analysis dictates that at high concentrations of acid the dominant solution species are $[MoH_3(CCHBu^t)(dppe)_2]^+$ and $[MoH_4(CCBu^t)(dppe)_2]^+$. This is also reflected in the spectrophotometric analysis of the absorbance *vs.* time traces. Careful inspection of these curves reveals that the initial absorbance varies with the concentration of HCl such that at low concentrations the initial absorbance is that of $[MoH_3(CCBu^t)(dppe)_2]$, whilst at high concentrations the initial absorbance is markedly smaller. Analysis of the way in which this initial absorbance varies with the concentration of HCl, as shown in Table 2, gives $(K_1 + K_2) = 26.8 \pm 5.0$ dm^3 mol^{-1} in excellent agreement with the value derived from the kinetic analysis. It is worth emphasising that this spectrophotometric analysis demonstrates, unambiguously, that the first stage corresponds to the consumption of 1 mole equivalent of HCl.

Since the formation of both $[MoH_3(CCHBu^t)(dppe)_2]^+$ and $[MoH_4(CCBu^t)(dppe)_2]^+$ occurs within the dead-time of the stopped-flow apparatus, even at the lowest concentration of HCl used, we can estimate that both k_1 ($=K_1k_{-1}$) and k_2 ($=K_2k_{-2}$) $\geqslant 1 \times 10^5$ dm^3 mol^{-1} s^{-1}, whilst the results from the earlier study on $[MoH_2(CCBu^t)_2(depe)_2]$ indicate $k_1 \approx 500k_2$.

Protonation at the metal is a proposal that can adequately be accommodated by the kinetics and is able to rationalise why an alkyne is formed in the reaction of $[MoH_3(CCBu^t)(dppe)_2]$ with HCl, rather than the usual formation of an alkylidyne complex, but spectroscopic evidence for this proposal is necessary.

The visible absorption spectrum of the equilibrium mixture of $[MoH_3(CCHBu^t)(dppe)_2]^+$ and $[MoH_4(CCBu^t)(dppe)_2]^+$ (formed within the dead time of the stopped-flow apparatus) is shown in Fig. 2. Since the individual values of K_1 or K_2 are unknown, the relative amounts of $[MoH_3(CCHBu^t)(dppe)_2]^+$ and $[MoH_4(CCBu^t)(dppe)_2]^+$ in this equilibrium mixture cannot be calculated, and hence the major solution species is unknown. However, from studies on the reaction of $[MoH_3(CCBu^t)(dppe)_2]$ with $HBF_4{\cdot}OEt_2$ (see later discussion), where only protonation at the C_β site of the alkynyl ligand occurs, it is clear that the spectrum in Fig. 2 is predominantly that of $[MoH_3(CCHBu^t)(dppe)_2]^+$.

An intermediate has also been detected in the reaction of $[MoH_3(CCBu^t)(dppe)_2]$ with HCl using $^{31}P\text{-}\{^1H\}$ NMR spectroscopy at -80 °C. It exhibits a singlet at δ -65 as shown in Fig. 2, which progressively grows in intensity as the signal due to $[MoH_3(CCBu^t)(dppe)_2]$ collapses, and then decreases in intensity as the peaks associated with the product, $[MoH_2Cl_2(dppe)_2]$, appear. The spectrum of this intermediate demonstrates that it is a single species and that all the phosphorus atoms in this complex are magnetically equivalent. It seems most likely that this intermediate is $[MoH_3(\eta^2\text{-}CHCBu^t)(dppe)_2]^+$. It seems unlikely that the sharp resonance at δ -65 represents the equilibrium protonation mixture between $[MoH_3(CCBu^t)(dppe)_2]$, $[MoH_3(CCHBu^t)(dppe)_2]^+$ and $[MoH_4(CCBu^t)(dppe)_2]^+$, since if this were the case we

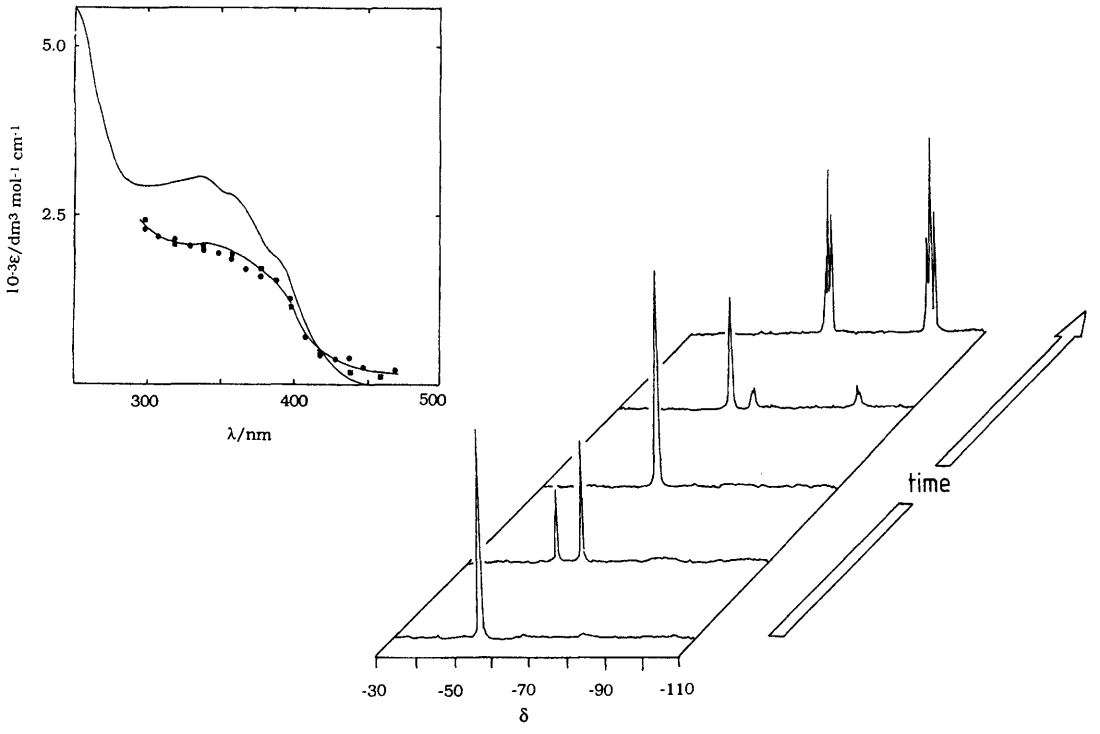

Fig. 2 The ^{31}P-$\{^1H\}$ NMR spectral time course at −80 °C, showing the appearance followed by the disappearance of the intermediate and accumulation of the product, $[MoH_2Cl_2(dppe)_2]$, formed in the reaction between $[MoH_3(CCBu^t(dppe)_2]$ (10 mmol dm^{-3}) and an excess of anhydrous HCl (100 mmol dm^{-3}). The insert shows visible absorption spectra of $[MoH_3(CCBu^t)(dppe)_2]$ and the intermediate $[MoH_3(CCHBu^t)(dppe)_2]^+$, formed in the reactions with HCl (●) or HBF_4 (■)

Table 2 Spectrophotometric determination of the sum of the equilibrium constants for protonation of the alkynyl residue (K_1) and the metal (K_2) in the reaction of $[MoH_3(CCBu^t)(dppe)_2]$ (0.1 mmol dm^{-3}) with anhydrous HCl in thf at 25.0 °C, I = 0.1 mol dm^{-3} ($[NBu^n_4]BF_4$), λ = 450 nm

[HCl]/mmol dm^{-3}	Absorbance	$(K_1 + K_2)$*/dm^3 mol^{-1}
5.0	0.130	24.5
10.0	0.120	27.9
20.0	0.108	26.7
40.0	0.094	25.0
60.0	0.084	26.0
80.0	0.078	25.8
100.0	0.070	31.8
		Average = 26.8 ± 5.0

* $(K_1 + K_2) = \{[MoH_3(CCHBu^t)(dppe)_2^+]_e + [MoH_4(CCBu^t)(dppe)_2^+]_e\}/[MoH_3(CCBu^t)(dppe)_2]_e[HCl]$ where the subscript 'e' denotes the 'equilibrium' concentration. The equilibrium concentrations were calculated spectrophotometrically using Beer's law and the following molar absorption coefficients: $\varepsilon\{[MoH_3(CCBu^t)(dppe)_2]_e\} = 1.4 \times 10^3$; $\varepsilon\{[MoH_3(CCHBu^t)(dppe)_2^+]_e + [MoH_4(CCBu^t)(dppe)_2^+]_e\} = 4.8 \times 10^2$ dm^3 mol^{-1} cm^{-1}. These values were calculated from the initial absorbance of the stopped-flow absorbance *vs.* time trace at [HCl] = 0.0 and 200 mmol dm^{-3} respectively.

would expect that, under the conditions these experiments were performed, the resonance attributable to the starting material, $[MoH_3(CCBu^t)(dppe)_2]$, would be present or a broadened average resonance would be observed. Certainly, at the concentrations used in this NMR spectroscopy experiment, we can calculate that at 25.0 °C about 40% of the solution species is $[MoH_3(CCBu^t)(dppe)_2]$. Assuming that the protonation reactions are exothermic it would be expected that at −80 °C the amount of $[MoH_3(CCBu^t)(dppe)_2]$ would be greater than this.

The proton-coupled ^{31}P NMR spectrum of this intermediate is a broad signal with no discernible fine structure. The intermediate is insufficiently long-lived and the solubility too low at −80 °C to obtain ^{13}C NMR spectra and hence obtain information about the identity of the hydrocarbon residue. These spectroscopic limitations mean that we have to rely on kinetic information to establish the identity of the intermediates.

Evidence that this first stage of the reaction between HCl and $[MoH_3(CCBu^t)(dppe)_2]$ involves protonation at the metal comes from studies using DCl. In the presence of DCl the same rate law as with HCl [equation (4)] is observed with $k_4^D K_2^D = (2.1 \pm 0.1) \times 10^2$ dm^3 mol^{-1} s^{-1} and $(K_1^D + K_2^D) = 15.7 \pm 3.0$ dm^3 mol^{-1}. Consequently the isotope effects are $k_4^H K_2^H / k_4^D K_2^D = 2.87 \pm 0.3$ and $(K_1^H + K_2^H)/(K_1^D + K_2^D) = 1.15 \pm 0.50$. Since, as expected, the isotope effect associated with the equilibrium constants is small,[10] we can estimate that k_4^H / k_4^D = *ca.* 2.5. This significant primary isotope effect associated with the intramolecular coupling step is consistent only with initial protonation at the metal. If the latter is a rapid equilibrium process then, in the reactions with DCl, exchange of the hydride ligands for deuterium will be complete before the coupling step which produces the co-ordinated alkyne. Consequently in the reactions of $[MoH_3(CCBu^t)(dppe)_2]$ with DCl the migrating group is not a hydride but a deuterium atom, and this gives rise to the primary isotope effect observed for the k_4 step.

That the hydride ligands exchange for deuterium is confirmed by mass spectrometric studies which show that in the reactions with DCl the dominant gaseous products are HD and D_2.

Second stage: release of the products. The second stage of the absorbance *vs.* time curve must be associated with the following elementary reactions: the addition of a proton to $[MoH_3(\eta^2\text{-}CHCBu^t)(dppe)_2]^+$; dissociation of both dihydrogen and alkyne and binding of chloride to form $[MoH_2Cl_2(dppe)_2]$. Consideration of the mechanism in Scheme 2 indicates that the rate law (5) is associated with the second stage assuming that the protonation step is a rapidly established equilibrium (K_5), dissociation of either dihydrogen or alkyne is rate-limiting (k_6) and that $[MoH_3(CCBu^t)(dppe)_2]$ is converted stoichiometrically into $[MoH_3(\eta^2\text{-}CHCBu^t)(dppe)_2]^+$ in the first stage of

$$\frac{d[MoH_2Cl_2(dppe)_2]}{dt} = \frac{k_6K_5[HCl][MoH_3(CCBu^t)(dppe)_2]}{1 + K_5[HCl]} \quad (5)$$

the reaction. Comparison of equations (2) and (5), using the experimentally determined values of a and b, gives $K_5 = 2.46 \pm 0.3$ dm^3 mol^{-1} and $k_6 = 2.0 \pm 0.3$ s^{-1}.

The fundamental mechanistic problem for this stage of the reaction is whether k_6 corresponds to dissociation of dihydrogen or alkyne. Equation (5) cannot distinguish between these two possibilities. Quantitative analysis of the time course for the release of dihydrogen using GLC, as shown in Fig. 3, demonstrates that dihydrogen is evolved at a rate predicted by equation (5). The detection of these relatively low concentrations of dihydrogen leads to a degree of scatter in these data but this experiment demonstrates unambiguously that dihydrogen is evolved after the addition of two protons, but does not prove that this occurs before the alkyne since k_6 is the rate-limiting step for the release of both alkyne and dihydrogen, irrespective of the order in which they dissociate from the metal. Kinetic studies with DCl do, however, indicate strongly that dihydrogen is released before the alkyne. When the reaction is studied with DCl the rate law (5) is obeyed with $k_6^D = 1.25 \pm 0.20$ s^{-1} and $K_5^D = 2.86 \pm 0.30$ dm^3 mol^{-1}. The derived isotope effects are $K_5^H/K_5^D = 0.92 \pm 0.15$ and $k_6^H/k_6^D = 1.6 \pm 0.2$. The small value for K_5^H/K_5^D is consistent with this being an equilibrium isotope effect,[10] whilst the significant primary isotope effect associated with the k_6 step is consistent with rate-limiting dissociation of dihydrogen. That k_6 is associated with a primary isotope effect is a consequence of the initial protonation site being the metal. As discussed above, in the reactions with DCl, rapid, equilibrium protonation at the metal leads to exchange of the hydride ligands on $[MoH_3(CCBu^t)(dppe)_2]$ with deuterons, so that ultimately dissociation of dideuterium occurs from the species $[MoD_4(\eta^2\text{-}CDCBu^t)(dppe)_2]^{2+}$. If the k_6 step is associated with dissociation of the alkyne it is difficult to see how this would be associated with a primary isotope effect.

Another indication that dihydrogen is labilised preferentially from $[MoH_4(\eta^2\text{-}CHCBu^t)(dppe)_2]^{2+}$ comes from considering the species that would be generated immediately after dissociation of either dihydrogen or alkyne, as shown in equations (6) and (7) respectively. Preferential loss of the alkyne

$$[MoH_4(\eta^2\text{-}CHCBu^t)(dppe)_2]^{2+} \longrightarrow [MoH_2(\eta^2\text{-}CHCBu^t)(dppe)_2]^{2+} + H_2 \quad (6)$$

$$[MoH_4(\eta^2\text{-}CHCBu^t)(dppe)_2]^{2+} \longrightarrow [MoH_4(dppe)_2]^{2+} + Bu^tCCH \quad (7)$$

from $[MoH_4(\eta^2\text{-}CHCBu^t)(dppe)_2]^{2+}$ [equation (7)] would generate the species $[MoH_4(dppe)_2]^{2+}$. This intermediate is formed in the protonation reactions of $[MoH_4(dppe)_2]$[11] and has been shown to bind and activate a wide range of small molecules rapidly including dinitrogen, methyl isocyanide, azide, phenylacetylene, ethyl propiolate, carbon monoxide, methyl cyanide and carbon dioxide.[12,13] However, when $[MoH_3(CCBu^t)(dppe)_2]$ is treated with anhydrous HBr (5 mole equivalents) in the presence of an excess (10–1000 mole equivalents) of ethyl propiolate only $[MoH_2Br_2(dppe)_2]$ is formed [^{31}P-{^{1}H} NMR spectrum: δ −75 (triplet), −100 (triplet), J_{PP} = 12.7 Hz. ^{1}H NMR spectrum: δ −5.6 (quintet), J_{PH} = 54 Hz, MoH].[14] Previous studies have shown that in reactions involving the intermediate, $[MoH_4(dppe)_2]^{2+}$, then $[MoH_2Br(CHCHEt)(dppe)_2]$ [^{31}P-{^{1}H} NMR: δ −55.65 (singlet). ^{1}H NMR: δ −5.6 (quintet), J_{PH} = 52 Hz, MoH][3] is produced. In summary, both kinetic isotope experiments and trapping experiments are consistent with dihydrogen being released from the metal before the alkyne.

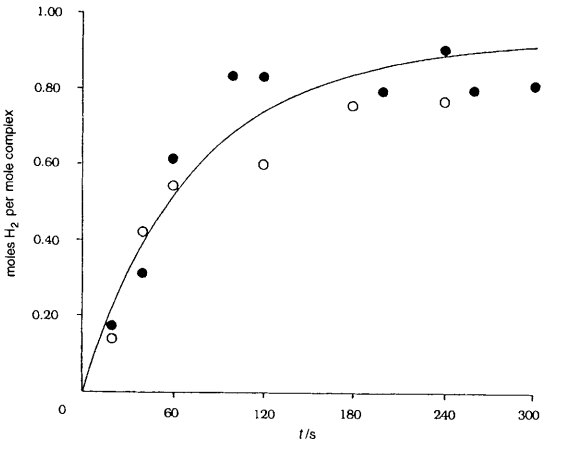

Fig. 3 Time course of the evolution of dihydrogen (monitored using GLC) in the reaction of $[MoH_3(CCBu^t)(dppe)_2]$ (1.0 mmol dm^{-3}) with anhydrous HCl (5.0 mmol dm^{-3}) in thf at 25.0 °C. The curve is that defined by equation (5). The open and closed symbols are the results from two independent experiments, and give some indication of the error

It is clear from the mechanism shown in Scheme 2 that the conversion of $[MoH_3(CCBu^t)(dppe)_2]$ into $[MoH_3(\eta^2\text{-}CHCBu^t)(dppe)_2]^+$ involves eight- or nine-co-ordinate, co-ordinatively saturated, eighteen-electron species. However, the high formal co-ordination number associated with these complexes is a consequence of the relatively large number of sterically undemanding hydride ligands present in the co-ordination sphere and hence does not represent a major steric problem. However, after the second protonation $[MoH_4(\eta^2\text{-}CHCBu^t)(dppe)_2]^{2+}$ is formed and both the increased steric congestion and the dicationic nature of this species renders it labile to dissociation. It is only after the dissociation of dihydrogen from this intermediate and formation of $[MoH_2(\eta^2\text{-}CHCBu^t)(dppe)_2]^{2+}$ that the metal becomes co-ordinatively unsaturated. Thus it is only at this stage that chloride ion can bind to the metal.

Protonation of the metal *versus* protonation of the alkynyl ligand

In contrast to this study, previous synthetic studies have shown that the reaction of $[MoH_3(CCBu^t)(dppe)_2]$ with an excess of $HBF_4{\cdot}OEt_2$ in thf produces an alkylidyne[6] as shown in equation (8). If our mechanism for reaction (1), shown in

$$[MoH_3(CCBu^t)(dppe)_2] \xrightarrow{HBF_4\cdot OEt_2} [MoF(CCH_2Bu^t)(dppe)_2]^+ \quad (8)$$

Scheme 2, is correct, and in particular the proposed competitive protonation of metal and alkynyl ligand, then the formation of this alkylidyne complex must be slower than that of $[MoH_3(\eta^2\text{-}CHCBu^t)(dppe)_2]^+$. Unfortunately a full quantitative comparison between the kinetics of reactions (1) and (8) is not possible since the latter clearly involves not only protonation and substitution steps, but also the complex becomes oxidised, presumably by acid.

We have studied the kinetics of reaction (8) on the stopped-flow apparatus. This is most convenient at λ = 510 nm, where the red product, $[MoF(CCH_2Bu^t)(dppe)_2]^+$, absorbs. At this wavelength the reaction between $[MoH_3(CCBu^t)(dppe)_2]$ and $HBF_4{\cdot}OEt_2$ occurs in two distinct stages: an initial absorbance increase corresponding to the formation of an intermediate, which is complete within the dead-time of the apparatus (2 ms), followed by an exponential absorbance increase, complete within 5 s. The exponential trace indicates a first-order dependence on the concentration of $[MoH_3$-

$(CCBu^t)(dppe)_2]$ and this was confirmed in studies where the complex concentration was varied in the range 0.025–0.2 mmol dm^{-3} with $[HBF_4]$ = 20 mmol dm^{-3}. Under these conditions the observed rate constant did not vary, $k_{obs} = 1.2 \pm 0.2\ s^{-1}$. The reaction was independent of the concentration of acid over the range $[HBF_4]$ = 1–30 mmol dm^{-3}, $k_{obs} = 1.2 \pm 0.2\ s^{-1}$.

The visible absorption spectrum of the intermediate formed in the reaction with $HBF_4{\cdot}OEt_2$ is identical to that of the intermediate formed in the reactions with HCl, as shown in Fig. 2. Now the studies with HCl indicate that, if protonation occurs at the metal, formation of $[MoH_3(\eta^2\text{-}CHCBu^t)(dppe)_2]^+$ ensues at a rate limited by an intramolecular reductive coupling of a hydride and alkynyl ligand (k_4), and this step commits the system to the production of alkyne. We can estimate that $k_4 \geqslant 33\ s^{-1}$, from equation (4), since $(K_1 + K_2) = 18\ dm^3\ mol^{-1}$ and hence $K_2 \leqslant 18\ dm^3\ mol^{-1}$. Since the measured limiting rate constant for the formation of *trans*-$[MoF(CCH_2Bu^t)(dppe)_2]^+$ ($k = 1.2\ s^{-1}$) is much slower than k_4, we can conclude that $HBF_4{\cdot}OEt_2$ does not protonate the metal, possibly because of the steric bulk of the acid which in this low relative permittivity, aprotic solvent is a weak acid. Hence, the electronic spectrum in Fig. 2 is predominantly that of $[MoH_3(CCHBu^t)(dppe)_2]^+$ both in the studies with HCl and $HBF_4{\cdot}OEt_2$, and in the reaction with HCl only small amounts of $[MoH_4(CCBu^t)(dppe)_2]^+$ are generated.

The kinetics of the formation of the alkylidyne in the reaction with $HBF_4{\cdot}OEt_2$ is consistent with the top pathway shown in Scheme 2. After protonation at the alkynyl ligand the system has to await the slow coupling of two hydride ligands or possibly loss of dihydrogen, $k_3 = 1.2 \pm 0.2\ s^{-1}$. Subsequently, $[MoH(CCHBu^t)(dppe)_2]^+$ rapidly forms $[MoF(CCH_2Bu^t)(dppe)_2]^+$ by a pathway we cannot define from experimental observations but presumably involves binding of fluoride ion (derived from the BF_4^-), further protonation of the remote carbon atom and a formal release of hydrogen atom from the metal.

It is clear from this discussion that, *irrespective of the acid, the maximum rate at which the alkylidyne complex can be produced is that defined by* k_3. The study of reaction (8) now permits a quantitative description of the product distribution for reaction (1).

The amount of alkylidyne complex produced in the reaction with HCl is defined by the rate of formation of $[MoH(CCHBu^t)(dppe)_2]$, and is given by the expression (9). Similarly the

$$\frac{d[MoH(CCHBu^t)(dppe)_2^+]}{dt} = \frac{k_3K_1[HCl][MoH_3(CCBu^t)(dppe)_2]}{1 + (K_1 + K_2)[HCl]} \quad (9)$$

amount of alkyne produced in the same reaction is defined by the rate of formation of $[MoH_3(\eta^2\text{-}CHCBu^t)(dppe)_2]^+$ as given in equation (4). Hence the proportion of the reactant which will go on to produce free alkyne in the reaction with HCl is given by equation (10). From the kinetic analyses presented in this paper, the values of $k_4K_2 = 6.0 \times 10^2\ dm^3\ mol^{-1}\ s^{-1}$ and $k_3 = 1.2\ s^{-1}$ are known, and in addition since $(K_1 + K_2) = 18.0$, $K_1 \leqslant 18.0$. Substituting these values into equation (10)

$$\text{Percentage of alkyne formed} = \frac{k_4K_2}{k_4K_2 + k_3K_1} \times 100 \quad (10)$$

shows that in the reaction with HCl the amount of alkyne produced is (*i*) independent of the concentration of acid and (*ii*) formed in greater than 97% yield. Both these features are observed experimentally.

Conclusion

Previous studies have shown that the protonation of alkynyl complexes normally occurs at the C_β atom of the alkynyl ligand and results in the formation of an alkylidyne complex. We have shown in this paper that, under certain conditions, protonation of an alkynyl complex can result in the formation of an alkyne. The origins of these different reactivities of alkynyl complexes towards protons are: (*i*) the ability of alkynyl complexes to protonate at either the ligand (to give alkylidyne complexes) or the metal (to give alkynes) and (*ii*) the rapidity with which these protonated species undergo intramolecular hydrogen–hydrogen or hydrogen–alkynyl reductive-coupling reactions, respectively. These coupling reactions are an essential prerequisite for further protonation and hence product formation in complexes where the metal is in its highest formal oxidation state. *In systems where protonation of both the alkynyl ligand and the metal can occur the pathway which ultimately dominates the reaction is dictated not by the relative rates of protonation of the alkynyl and metal sites or the thermodynamics associated with these protonations, but by the subsequent rates of intramolecular coupling and dissociation reactions leading to the formation of alkylidyne or alkyne.*

References

1 R. A. Henderson, *Angew. Chem., Int. Ed. Engl.*, 1996, **35**, 946 and refs. therein.
2 R. A. Henderson, S. Martyr and K. E. Oglieve, *An. Quim., Int. Ed.*, 1996, in the press.
3 R. A. Henderson, *J. Chem. Soc., Dalton Trans.*, 1982, 917.
4 J. H. Espenson, *Chemical Kinetics and Reaction Mechanisms*, McGraw-Hill, New York, 1981, ch. 2.
5 A. J. L. Pombeiro, A. Hills, D. L. Hughes and R. L. Richards, *J. Organomet. Chem.*, 1990, **398**, C15.
6 M. A. N. D. A. Lemos, A. J. L. Pombeiro, D. L. Hughes and R. L. Richards, *J. Organomet. Chem.*, 1992, **434**, C6.
7 R. A. Henderson and K. E. Oglieve, *J. Chem. Soc., Dalton Trans.*, 1993, 3431.
8 R. A. Henderson and K. E. Oglieve, *J. Chem. Soc., Dalton Trans.*, 1994, 767 and refs. therein.
9 R. G. Wilkins, *Kinetics and Mechanism of Reactions of Transition Metal Chemistry*, 2nd edn., VCH, Weinheim, 1991, p. 23.
10 R. P. Bell, *The Proton in Chemistry*, 2nd edn., Chapman and Hall, London, 1973, ch. 11 and refs. therein.
11 R. A. Henderson, *J. Chem, Soc., Chem. Commun.*, 1987, 1670.
12 R. Ellis, R. A. Henderson, A. Hills and D. L. Hughes, *J. Organomet. Chem.*, 1987, **333**, C6.
13 N. Kashef and R. L. Richards, *J. Organomet. Chem.*, 1989, **365**, 309.
14 K. E. Oglieve and R. A. Henderson, *J. Chem. Soc., Dalton Trans.*, 1991, 3295.

Received 8*th March* 1996; *Paper* 6/01652I